



# Organic-inorganic hybrid network constructed in polypropylene matrix and its reinforcing effects on polypropylene composites

Han Zhu<sup>1</sup>, MingLiang Du<sup>1,2</sup>, CongSheng Xu<sup>1</sup>,  
 XianMing Zhang<sup>1,2</sup> and YaQin Fu<sup>1,2</sup>

## Abstract

A facile approach was proposed to improve the mechanical properties of the polymer composites by organic-inorganic hybrid networks assembled via hydrogen bonding between halloysite nanotubes and organic hydrogen bonding coupler. Organic hydrogen bonding couplers were incorporated to the polypropylene composites and the hybrid networks were *in situ* constructed in the process of the fabricating of the composites. The investigations suggest that the formation of hybrid network can remarkably improve the mechanical properties of the composites, mainly including the tensile strength, flexural properties. In addition, the hydrogen bonds between organic hydrogen bonding coupler and halloysite nanotubes and the constructed organic-inorganic hybrid networks were characterized by Fourier transform infrared spectroscopy and X-ray photoelectron spectroscopy. The results show that the absorption of Si-O of the Fourier transform infrared spectroscopy spectra and the binding energy of the Si and Al atoms of the X-ray photoelectron spectroscopy spectra changed to some extent, indicating the existence of hydrogen bonds between organic hydrogen bonding coupler and halloysite nanotubes. Dynamic mechanical studies suggest the existence of the hybrid networks in the polypropylene matrix.

## Keywords

Hydrogen bond, hybrid networks, polypropylene, composites, mechanical properties

## Introduction

In recent years, preparing all kinds of excellent performance polymer composites with polymer and fillers (mainly inorganic fillers) has become a very convenient and favored strategy in polymer science for their advantages such as more easily to be processed, higher thermal stability, lower cost and so on.<sup>1,2</sup> However, the compatibility between polymer and fillers may lead to the unsatisfied performance, which impedes the further application of the polymer/filler composites.<sup>3,4</sup> As a consequence, how to reinforce the polymer materials is always the emphasis in polymer science.<sup>5–7</sup>

In the present, many approaches have been taken for the reinforcement of polymer materials, such as fiber-reinforced composites, chemical modifications, reinforcement of composites with whiskers, hydrogen bonding bridged inorganics and so on.<sup>8–12</sup> Compared

with the conventional method such as utilizing coupling agents to improve the compatibility of the polymer/inorganic filler composites, hydrogen bonding bridged inorganics is a method irrespective of the low compatibility between inorganics and polymer materials.<sup>8</sup>

<sup>1</sup>Department of Polymer Materials and Engineering, Zhejiang Sci-Tech University, China

<sup>2</sup>Key Laboratory of Advanced Textile Materials and Manufacturing Technology, Ministry of Education, China

### Corresponding author:

MingLiang Du, Key Laboratory of Advanced Textile Materials and Manufacturing Technology, Ministry of Education, Hangzhou 310018, China.

Email: du@zstu.edu.cn

So far, the formation of filler network in polymer matrix have been reported by numerous researchers.<sup>13,14</sup> Although the reinforcing effects of inorganics on plastics are widely reported, the reinforcement of polypropylene (PP) via inorganics network has not been fully recognized and the development of the reinforcing strategy irrespective of the polarity discrepancy is highly desirable. Traditionally, the interface and compatibility play a crucial role in improving the mechanical properties of plastics/inorganic filler composites. Recently, another new strategy was proposed irrespective of the low compatibility between inorganics and thermoplastics.<sup>15–17</sup> Compared with the conventional method to improve the compatibility of the plastics/inorganic filler composites, this method exhibits much effective reinforcing effects and the process is much facile.

In present work, we intend to further verify the effectiveness of the strategy in reinforcing PP through hybrid network assembly of HNTs during the process. Three hydrogen bonding coupler (HBC), tea polyphenols (TP), Zein and polylactic acid (PLA), were incorporated to form hybrid networks with halloysite nanotubes (HNTs) through hydrogen bonds. The effectiveness of this strategy to PP was also examined.

## Experimental

### Materials

PP granules were purchased from Basel Company. The melt flow index was determined as 2.84 g/10 min (after ISO-1133: 1997(E)). HNTs were collected from Hubei Province, China. The Brunauer-Emmett-Teller (BET) surface area of the HNTs was determined as 50.45 m<sup>2</sup>/g with a specific surface area and porosity analyzer, ASAP 2020 of Micromeritics. TP, Zein and PLA were employed as HBC for the construction of organic-inorganic hybrid networks. TP was provided by Xuancheng Baicao Plant Industry and Trade Co., Ltd. TP are a group of water-soluble polyphenols richly deposited in plants, belonging to the flavonoid family, and mainly consist of epicatechin, epicatechin gallate, epigallocatechin and epigallocatechin gallate, in which the epigallocatechin gallate makes up about 45% of the total TP. Zein (F4000), with a molecular weight of 35 kDa, was purchased from Shanghai Jinhui Biotechnology Co., Ltd. PLA was a commercial product (Zhejiang Haisheng biological materials Co., Ltd., China) with high optical purity with about 98% L-lactide content, density 1.24 g/cm<sup>-3</sup>, weight-average molecular weight ( $M_w$ ) 250 kDa, polydispersity 1.70 and the glass transition temperature and melting point of 60.48 and 166.40°C, respectively. In the

manuscript, TP, Zein and PLA all consist of multiple hydroxyl groups and the hydroxyl groups can form hydrogen bonds with the surface hydroxyl groups of HNTs to construct hybrid networks.

### Preparation of the PP/HNTs composites

In the present investigation, all raw materials were mixed with a twin-screw extruder. The screw diameter of the twin-screw-extruder is 35 mm and the screw speed was 100 r/min. The temperatures profile from the barrel to the die were 175/185/195/200/200/200/200/200/200/230°C, respectively, which are shown in Table 1.

The pelletized granules were dried in vacuum oven under 80°C for 6 h. Then the granules were injection molded to the specimens for characterizations at 200°C. The composition of the PP/HNTs/HBC composites is shown in Table 2.

### Characterizations

**Transmission electron microscopy.** The HNTs were dissolved in diluted water solution and respectively dropped on the ultra-thin carbon-coated copper grid and dried under an infrared lamp for 5 min. The images were acquired using a JSM-2100 transmission electron microscopy (TEM, JEOL, Japan) at an accelerating voltage of 200 kV.

**Scanning electron microscopy.** The HNTs powders were spread on the conducting adhesive and the images were acquired using a LEO 1530 VP scanning electron microscopy (SEM) machine.

**Mechanical properties determinations.** Instron 3367 universal testing machine was used to perform the tensile, flexural and impact testing of PP/HNTs composites according to the standards of ISO 527-93, ISO 178-93 and ISO 180-93, respectively.

**Dynamic mechanical measurements.** Dynamic mechanical behavior measurements of all the PP, PP/HNTs and PP/HNTs/TP composites were performed on a DMA 242 dynamic analyser provided by Netzsch Company. The PP/HNTs composites were heated from -60 to 100°C at a ramping rate of 5°C/min in stretching mode.

**Attenuated total reflection-Fourier transform infrared spectroscopy.** HNTs powder, the organic HBC and the model mixtures of HNTs and the organic HBC were sheet-molded to small discs (about 2 mm thick and diameter about 10 mm). Then the little discs were analyzed by a Bruker Vector 33 spectrometer with the spectra changing from 4000 to 400 cm<sup>-1</sup> wave numbers.

**Table 1.** The temperatures profile from the barrel to the die

Heating position	I	II	III	IV	V	VI	VII	VIII	IX	X	die
Set temperature, °C	175	185	195	200	200	200	200	200	200	200	230
Actual temperature, °C	175 ± 3	185 ± 3	195 ± 3	200 ± 3	200 ± 3	200 ± 3	200 ± 3	200 ± 3	200 ± 3	200 ± 3	230 ± 3

HBC: hydrogen bonding coupler; HNTs: halloysite nanotubes; PP: polypropylene.

**Table 2.** The composition of the PP/HNTs/HBC composites. (HBC is TP, Zein and PLA, respectively)

Sample	PP content (phr)	HNTs content (phr)	HBC content (phr)
Pure PP	100	0	0
PP/HNTs	100	30	0
PP/HNTs/HBC	100	30	1
PP/HNTs/HBC	100	30	2.5
PP/HNTs/HBC	100	30	5
PP/HNTs/HBC	100	30	7.5
PP/HNTs/HBC	100	30	10

HBC: hydrogen bonding coupler; HNTs: halloysite nanotubes; PP: polypropylene; TP: tea polyphenols; PLA: polylactic acid.

**X-ray photoelectron spectroscopy.** X-ray photoelectron spectroscopy (XPS) spectra of HNTs, organic HBC and PP/HNTs/organic HBC composites were recorded by using an X-ray photoelectron spectrometer (Kratos Axis Ultra DLD) with an Aluminum (mono) K $\alpha$  source (1486.6 eV). The Aluminum K $\alpha$  source was operated at 15 kV and 10 mA. The vacuum degree was  $10^{-8}$  to  $10^{-7}$ , and the analysis area was about  $0.7 \times 0.3$  mm. For all the samples, a low-resolution survey run (0–1100 eV, pass energy = 160 eV) was performed. In order to obtain more information about the formation of hydrogen bonding, a high-resolution survey (pass energy = 48 eV) was performed at spectral regions relating to Si and Al.

## Results and discussion

### The reinforcing effects of HNTs hybrid network assembly on polypropylene composites

Figure 1(a) displays the TEM image of naturally occurring HNTs with abounded hydroxyls and the predominant form is a hollow tubular structure in the submicrometer range. The size of the inner and outer diameter of the halloysite tubules are approximately 15–20 and 40–50 nm, respectively, depending on the deposit condition.<sup>10,12–14</sup> As shown in Figure 1(b), the lumen length of the natural HNTs range from 500 to 2000 nm, and the high aspect ratio could afford more opportunities for the formation of hybrid networks. As reported previously, the typical crystal structure of HNTs consists of two types of hydroxyl groups with aluminol (Al-OH) groups in the internal surface and

Si-OH groups on the external surface.<sup>10,14,18</sup> Due to their outstanding properties, such as good dispersion in polymer matrix, larger ratio length, high strength, high modulus etc, HNTs have been disclosed as a new kind of ideal inorganic modifier to improve the mechanical and thermal properties of polymers.<sup>18,19</sup>

Figure 2 shows the different contents of HBC constructed hybrid networks with HNTs and the effect of various PP/HNTs/HBC ratios on mechanical properties of the PP/HNTs composites. It can be seen from Figure 2(a)–(e) that the flexural modulus, flexural strength and young's modulus of PP/HNTs composite both significantly increase to the maximum value and then decrease slowly with the increase of HBC contents. Compared with neat PP, the increment of the flexural modulus of PP/HNTs composites with 7.5 phr TP, Zeins and PLA adopted are 83%, 80% and 123%, respectively. Meanwhile, the increment of the flexural strength of PP/HNTs composite are 32%, 26% and 47%, respectively, with the content of TP, Zeins and PLA increasing to 5 phr. The increment of the young's modulus of PP/HNTs composite are 43%, 41% and 49%, respectively, with the content of TP, Zeins and PLA increasing to 7.5 phr. It is clear that PLA has a remarkable influence on the flexural modulus, young's modulus and flexural strength of PP/HNTs composite. Compared with TP and Zein, PLA possess longer molecular chains and more amounts of hydroxyls, which can offer more opportunity for the construction of hybrid networks via hydrogen bondings and the entanglement between HNTs and PP segments.<sup>20–22</sup> As previously reported, HBC possess multiple hydroxyls and the hydroxyls can be incorporated with HNTs

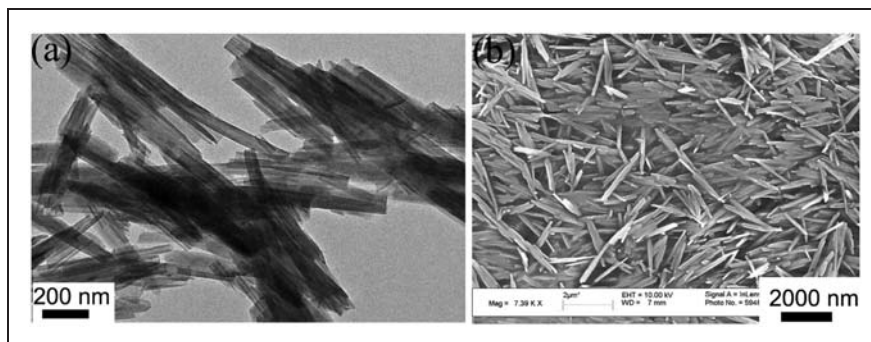


**Figure 1.** TEM and SEM images of the HNTs. TEM: Transmission electron microscopy; SEM: scanning electron microscopy; HNTs: halloysite nanotubes.

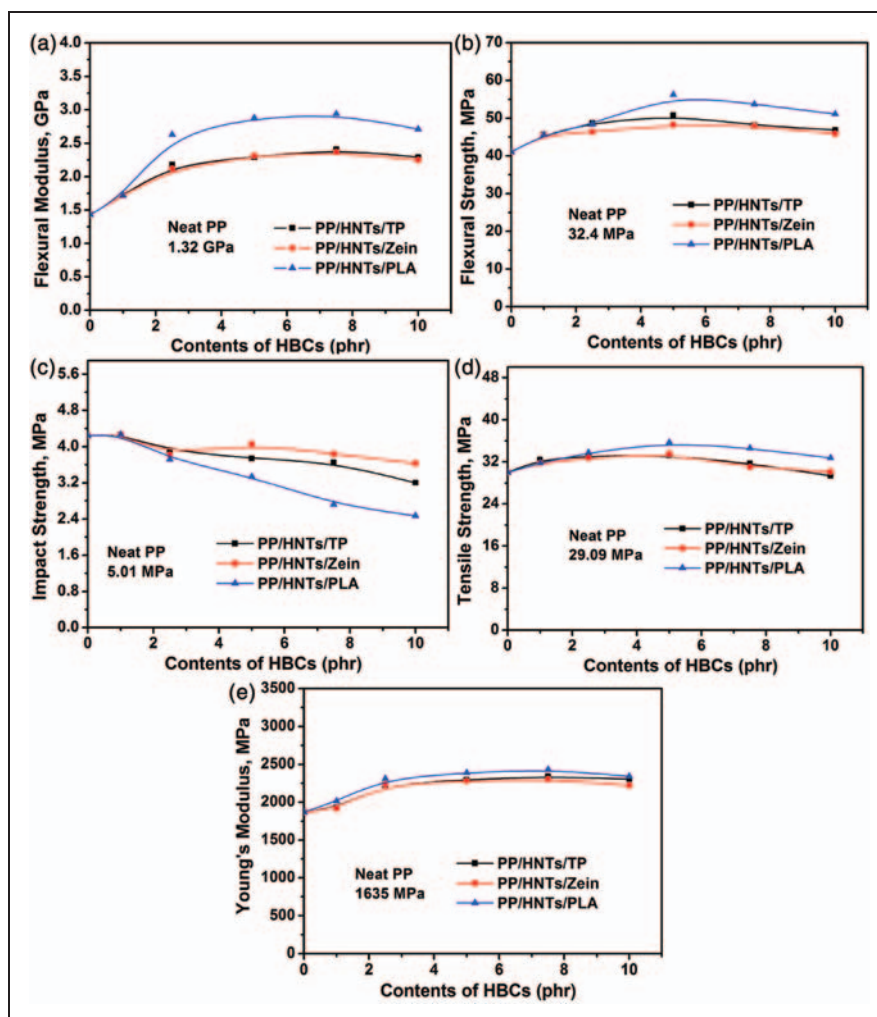


**Figure 2.** (a)–(e) Effects of the HBCs on mechanical properties of PP/HNTs (100/30) composite. HBC: hydrogen bonding coupler; PP: polypropylene; HNTs: halloysite nanotubes.

to form organic-inorganic hybrid networks through hydrogen bonds, which restricts the movement of HNTs and PP chains and then effectively increases the stiffness of PP/HNTs composite.<sup>19</sup> With the

incorporation of the HBC, the HNTs could be bridged via the hydrogen bonding between the hydroxyl groups on the surfaces of HNTs and functionalities of the organics. Once the organic-inorganic hybrid network

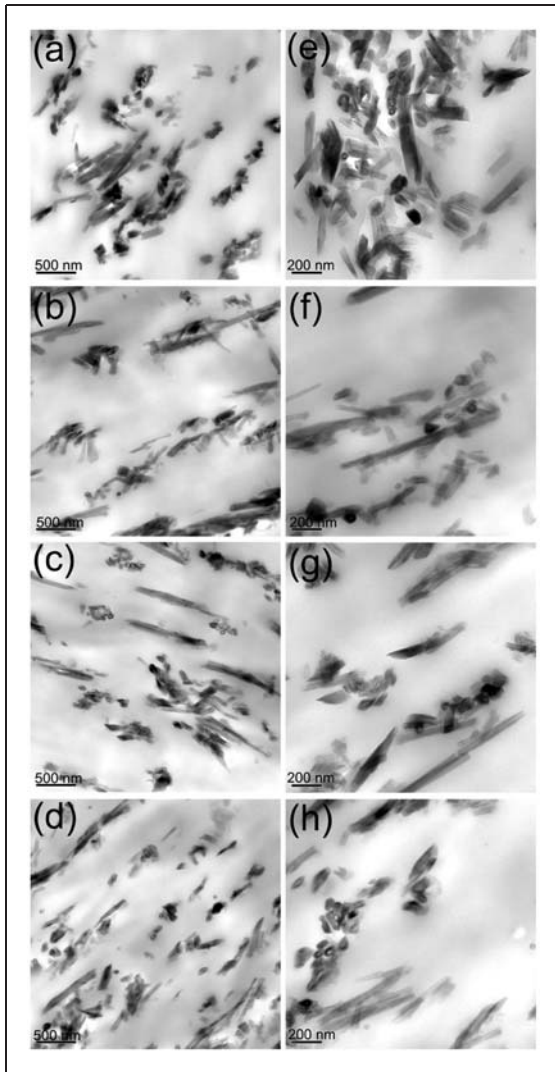


**Figure 3.** Morphology of ((a) and (e)) PP/HNTs (100/30) composites, ((b) and (f)) PP/HNTs/TP (100/30/5), ((c) and (g)) PP/HNTs/Zein (100/30/5) and ((d) and (h)) PP/HNTs/PLA (100/30/5). HBC: hydrogen bonding coupler; PP: polypropylene; HNTs: halloysite nanotubes; TP: tea polyphenols; PLA: polylactic acid.

constructed, the mobility of the PP chains at the interface will be therefore substantially restricted and consequently the composites show much higher rigidity. In addition, the hybrid network structure would be beneficial to the transfer of the loaded stress, which also should be responsible for the improved flexural properties and tensile strength. Figure 2(c) shows the effects of HBC on tensile strength of PP/HNTs composite. It is clear that the tensile strength also increases to the maximum value and then decreases slowly with the increase of HBC contents. It may due to the well dispersion of HNTs, the nano effect and the organic-inorganic hybrid networks formed by hydrogen bond between the HBC and HNTs. Figure 2(d) shows the effects of HBC on the impact strength of the PP/HNTs

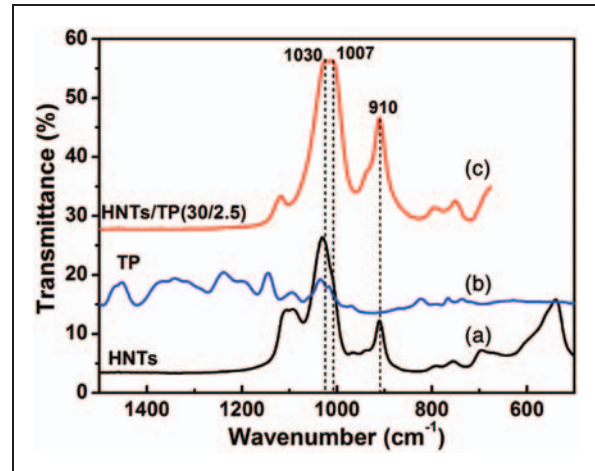


**Figure 4.** ATR-FTIR spectra of (a) HNTs, (b) TP and (c) HNTs/TP (HNTs:TP = 30/2.5). ATR-FTIR: attenuated total reflection-Fourier transform infrared spectroscopy; HNTs: halloysite nanotubes; TP: tea polyphenols.

composite. When 30 phr HNTs is incorporated, small decrease on the impact strength of the composite was obtained and with the inclusion of the increased amount of HBC, the impact strength decreased significantly. It may due to the formation of organic-inorganic hybrid networks and the hybrid networks can limit the free movement of PP chain, resulting in the reducing of the free volume of the PP chain segment. As discussed above, once the organic-inorganic hybrid networks constructed through hydrogen bonds, the movement of HNTs and PP chains were confined. When the composites are impacted, the dissipation of impact energy is less effective, leading to the deteriorated impact properties for all the composites. As a consequence, all the composites with the formation of hybrid networks show lower toughness.

The morphologies of the PP/HNTs composites and PP/HNTs/HBC composites are shown in Figure 3. Figure 3(a) and (e) show that the HNTs are dispersed disorderly in the PP matrix. The rings in the photos are the cross-sections of the tubes which are perpendicular to the observation direction. After the incorporation of TP, Zein and PLA, as indicated from Figure 3(b) to (h), the dispersion of HNTs in the composite is more uniform than the one without HBC. Compared with Figure 3(e)–(f), a close examination shows that for the PP/HNTs composites, the HNTs tend to self-aggregate via hydrogen bonding in the PP matrix because of the presence of surface hydroxyl groups of HNTs. Once the organics HBC containing hydrogen bonding functionalities are added, the hydroxyl groups on the surface of HNTs would combine with the HBC via hydrogen bonding, avoiding the self-aggregation of HNTs and consequently improving the dispersion of HNTs in PP matrix.

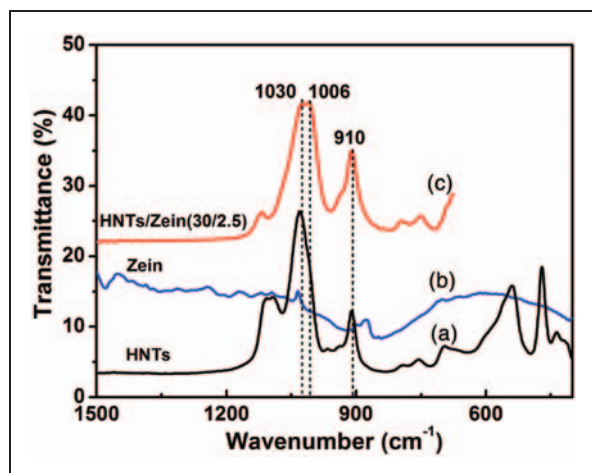


**Figure 5.** ATR-FTIR spectra of (a) HNTs, (b) Zein and (c) HNTs/Zein (HNTs/Zein = 30/2.5). ATR-FTIR: attenuated total reflection-Fourier transform infrared spectroscopy; HNTs: halloysite nanotubes.

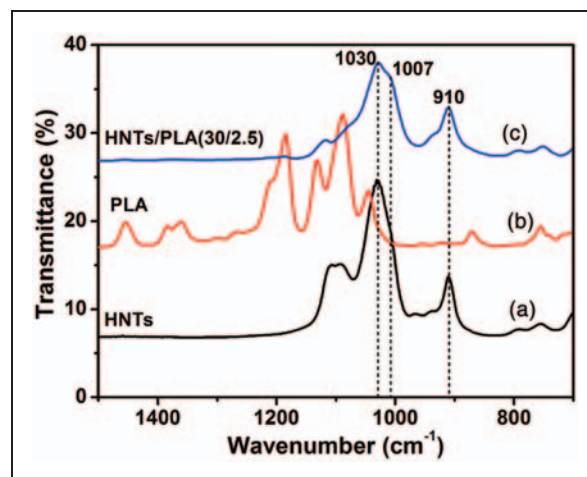


**Figure 6.** ATR-FTIR spectra of (a) HNTs, (b) PLA and (c) HNTs/PLA (HNTs/PLA = 30/2.5). ATR-FTIR: attenuated total reflection-Fourier transform infrared spectroscopy; HNTs: halloysite nanotubes; PLA: polylactic acid.

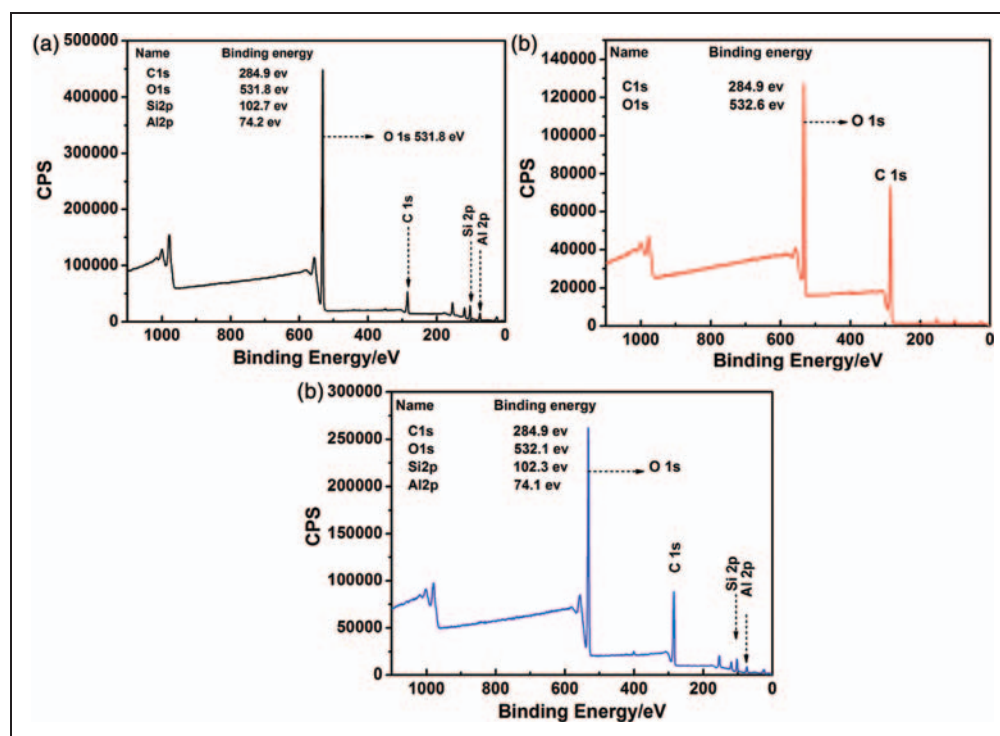


**Figure 7.** Low-resolution XPS spectra of (a) HNTs, (b) TP and (c) HNTs/TP. XPS: X-ray photoelectron spectroscopy; HNTs: halloysite nanotubes; TP: tea polyphenols.

### Characterizations of the formation of hybrid network between HNTs and TP

In the present work, we attempted to form organic-inorganic hybrid network constructed by hydrogen bonding interaction between HNTs and organic HBC. For this reason, all organic HBC used to form the hybrid network is required to contain hydrogen

bonding functionalities. In the present study, TP, Zein and PLA possessing large amount of hydroxyls (hydrogen bonding functionalities) were chosen to serve as organic HBC.

Figure 4–6 reveal the infrared spectra of several organic hydrogen ligands, HNTs and model compounds, respectively. Figure 4 shows the attenuated total reflection-Fourier transform infrared

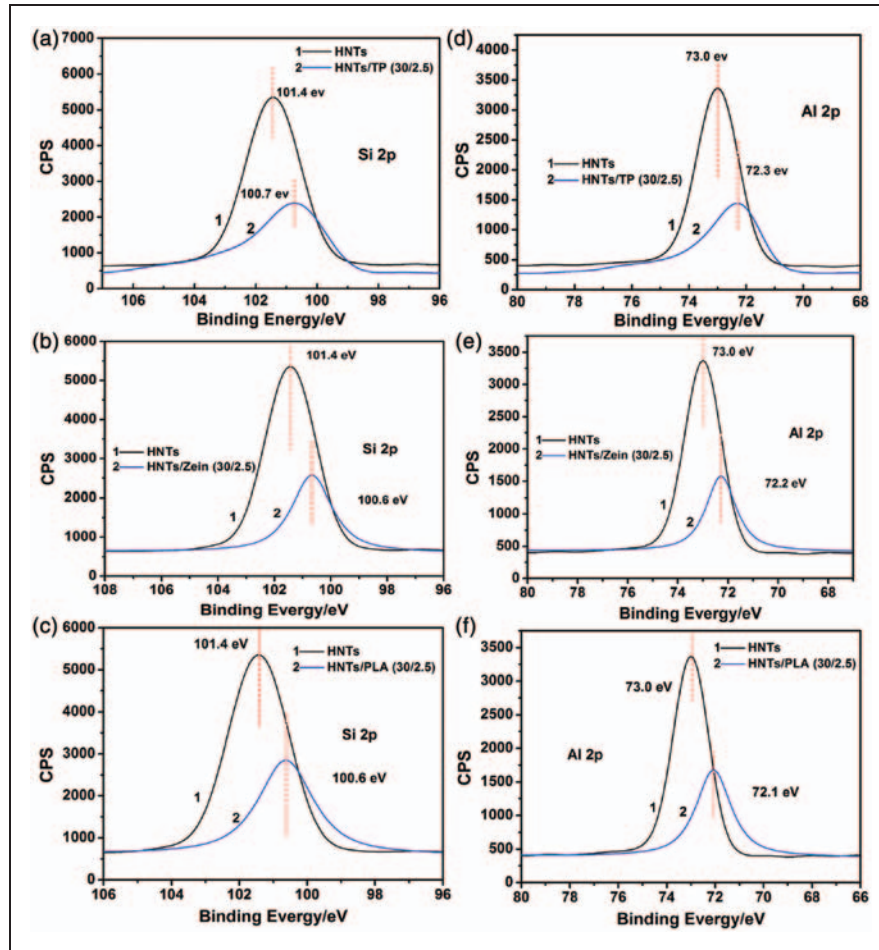


**Figure 8.** High-resolution Si 2p XPS spectra of (a) HNTs/TP, (b) HNTs/Zein and (c) HNTs/PLA. High-resolution Al 2p XPS spectra of (a) HNTs/TP, (b) HNTs/Zein and (c) HNTs/PLA. XPS: X-ray photoelectron spectroscopy; HNTs: halloysite nanotubes; TP: tea polyphenols; PLA: polylactic acid.

spectroscopy (ATR-FTIR) spectra of pure HNTs powders (curve a), TP powder (curve b) and the HNTs/TP composites (curve c). The characteristic peaks of HNTs that occurred at  $1030\text{ cm}^{-1}$  and  $910\text{ cm}^{-1}$  are ascribed to in-plane stretching of Si-O and the internal and external hydroxyls on the layered structure, which is caused by silicate and aluminum oxide octahedral. After the addition of TP, a new peak emerged at  $1007\text{ cm}^{-1}$ , which is attributed to the formation of hybrid networks through hydrogen bondings between HNTs and TP.

The similar results can also be obtained from the ATR-FTIR spectra of HNTs/Zein composites. From Figure 5, the Si-O and internal and external hydroxyls absorption peaks of HNTs are located at  $1030\text{ cm}^{-1}$  and  $910\text{ cm}^{-1}$ , respectively. Meanwhile, a new absorption peak located at  $1006\text{ cm}^{-1}$  in the HNTs/Zein composites indicates that the hydrogen bonding is presented in the HNTs/Zein compounds.

As shown in Figure 6, similarly, in the ATR-FTIR spectra of HNTs/PLA, a new peak emerged at  $1007\text{ cm}^{-1}$  is attributed to the formation of hybrid networks through hydrogen bondings between HNTs and PLA. In addition, the Si-O and internal and external hydroxyls absorption peaks of HNTs are located at  $1030\text{ cm}^{-1}$  and  $910\text{ cm}^{-1}$ , respectively. In conclusion, the FTIR characterizations confirm the formation of hybrid networks through hydrogen bonding between HNTs and HBCs.

XPS was further used to probe the surface chemical compositions and chemical state of the HNTs, TP and HNTs/HBC composites to confirm the formation of hydrogen bonding between HNTs and TP. As shown in Figure 7(a) and (b), the bonding energy of O 1s of the HNTs and TP are  $531.8\text{ eV}$  and  $532.6\text{ eV}$ , respectively. However, the O 1s spectra of HNTs/TP shown in Figure 7(c) indicates that the binding energy of O 1s have moved to  $532.1\text{ eV}$ .

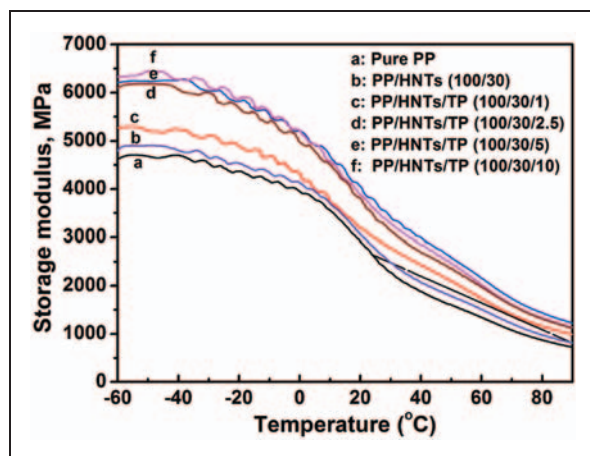


**Figure 9.** Effects of TP on storage modulus of PP/HNTs composites.

In order to further study the hydrogen bonding interaction between HNTs and HBC, high-resolution XPS spectra of Si and Al are obtained. As shown in Figure 8(a) and (d), compared with the binding energy of Si 2p and Al 2p in HNTs, respectively, there is a significant shift of 0.3 eV and 0.7 eV in HNTs/TP compounds, respectively, indicating that both Si and Al atoms are involved in the hydrogen bonding interaction between TP and HNTs.<sup>23</sup> Meanwhile, as shown in Figure 8, the bonding energy of Si 2p are 100.6 and 100.6 eV in HNTs/Zein and HNTs/PLA composites, respectively, while 101.4 eV in HNTs. In addition, the Al 2p spectra of HNTs/Zein and HNTs/PLA composites are 72.2 and 72.3 eV, respectively, while the Al 2p spectrum are 73.0 eV in HNTs. Both of the results reveal obvious shifts, indicating that the atom chemical environments of O and Si have obvious changes, indicating the formation of hydrogen bonds.<sup>24,25</sup>

It has been extensively investigated by many researchers that the formation of network structure in polymer matrix would lead to the variation of moduli.<sup>26–28</sup> Therefore, to further testify the existence of hydrogen bonding in the PP/HNTs matrix, the dynamic mechanical measurements of the composites were performed. In the present manuscript, TP is a kind of typical HBC, which possess many phenolic hydroxyl groups and offer much more opportunities for the construction of hybrid networks. In addition, the formation mechanism of hybrid networks among TP, Zein, PLA and HNTs is similar. Therefore, the PP/HNTs/TP composites were used to characterize the formation of the hybrid networks. Figure 9 shows the effects of TP on the storage modulus of PP/HNTs composite. Figure 9 reveals that the storage modulus increases to a certain extent when 1 phr, 2.5 phr and 5 phr TP are added to the PP/HNTs composite,

respectively. Furthermore, it can be seen that with the increase of the TP content from 1 phr to 2.5 phr, a sharp increase in the storage modulus of the composites is obtained. With the increasing of TP contents to 10 phr, a smaller improvement of the storage modulus of the composite is obtained. PP/HNTs composites with a series content of the TP show much higher storage modulus compared with neat PP/HNTs, which ascribe this phenomenon to the hydrogen bonding interaction between TP and HNTs in the PP matrix. Once the organic-inorganic hybrid network constructed via hydrogen bonding, the constitutive mobility of PP segments would significantly be restricted due to the entanglement between HNTs and PP segments. As a consequence, the storage modulus of PP/HNTs/TP composites is considerably increased. It is speculated that the formation of hybrid networks will effectively limit the free movement of PP chain, resulting in the increasing of the stiffness of the composite and storage modulus.

## Conclusions

Through the incorporation of certain organic HBC, PP/HNTs/HBC composites were prepared. In the composites, organic-inorganic hybrid networks were constructed by hydrogen bonding between HBC and HNTs, resulting in the significant increasing of the mechanical properties, such as flexural modulus, flexural strength and tensile strength. However, the impact strength gradually reduces with the inclusion of the increasing amounts of organic HBC, which is due to the formation of organic-inorganic hybrid networks. The formation of the organic-inorganic hybrid networks limits the free movement of PP chain, making the reducing free volume of the PP chain segment. The results of ATR-FTIR and XPS results demonstrate the strong hydrogen bonding interactions between HNTs and HBC. The dynamic mechanical behavior of composite materials indicates the formation of hybrid networks between HBC and HNTs with the incorporation of HBC.

## Funding

This research is funded by the National Natural Science Foundation of China (NSFC) (grant no. 50903072, 51243001) and Zhejiang Province Natural Science Foundation (grant no. Y4100197, Y4100534).

## References

- Porter D, Metcalfe E and Thomas MJK. Nanocomposite fire retardants-A review. *Fire Mater* 2000; 24: 45–52.
- Utracki LA and Kamal MR. Clay-containing polymeric nanocomposites. *Arab J Sci Eng* 2002; 27: 43–67.

3. Kim DH, Fasulo PD, Rodgers WR, et al. Structure and properties of polypropylene-based nanocomposites: Effect of PP-g-MA to organoclay ratio. *Polymer* 2007; 48: 5308–5323.
4. Molnara S, Pukanszky B, Hammer CO, et al. Impact fracture study of multicomponent polypropylene composites. *Polymer* 2000; 41: 1529–1539.
5. Costache MC, Wang DY, Heidecker MJ, et al. The thermal degradation of poly(methyl methacrylate) nanocomposites with montmorillonite, layered double hydroxides and carbon nanotubes. *Polym Advan Technol* 2006; 17: 272–280.
6. Miyagawa H, Misra M and Mohanty AK. Mechanical properties of carbon nanotubes and their polymer nanocomposites. *J Nanosci Nanotechnol* 2005; 5: 1593–1615.
7. Xia ZP, Yu JY, Cheng LD, et al. Scale effect on jute/cotton fibres and their blended yarns. *Fibers Text East Eur* 2009; 17: 43–45.
8. Du ML, Guo BC, Liu MX, et al. Reinforcing thermoplastics with hydrogen bonding bridged inorganics. *Physica B* 2010; 405: 655–662.
9. Jacob S, Suma KK, Mendez JM, et al. Reinforcing effect of nanosilica on polypropylene-nylon fibre composite. *Mat Sci Eng B* 2010; 168: 245–249.
10. Zhu H, Du ML, Zou ML, et al. Green synthesis of Au nanoparticles immobilized on halloysite nanotubes for surface-enhanced Raman scattering substrates. *Dalton Trans* 2012; 41: 10465–10471.
11. Xing DM, He GH, Hou ZJ, et al. Preparation and characterization of a modified montmorillonite/sulfonated polyphenylether sulfone/PTFE composite membrane. *Int J Hydrogen Energ* 2011; 36: 2177–2183.
12. Xu HHK, Quinn JB, Smith DT, et al. Effects of different whiskers on the reinforcement of dental resin composites. *Dent Mater* 2003; 19: 359–367.
13. Kashiwagi T, Du FM, Douglas JF, et al. Nanoparticle network reduced the flammability of polymer nanocomposites. *Nat Mater* 2005; 4: 928–933.
14. Dalmas F, Chazeau L, Gauthier C, et al. Large deformation mechanical behavior of flexible nanofiber filled polymer nanocomposites. *Polymer* 2006; 47: 2802–2812.
15. Du ML, Guo BC, Liu MX, et al. Formation of reinforcing inorganic network in polymer via hydrogen bonding self-assembly process. *Polym J* 2007; 39: 208–212.
16. Khalili SMR, Eslami Farsani R and Rafiezadeh S. An experimental study on the behavior of PP/EPDM/JUTE composites in impact, tensile and bending loadings. *J Reinf Plast Comp* 2011; 30: 1341–1347.
17. Bera M, Alagirusamy R and Das A. A study on interfacial properties of jute-PP composites. *J Reinf Plast Comp* 2010; 29: 3155–3161.
18. Liu MX, Guo BC, Zou QL, et al. Interactions between halloysite nanotubes and 2,5-bis(2-benzoxazolyl) thiophene and their effects on reinforcement of polypropylene/halloysite nanocomposites. 2008; 19: 205709–205718.
19. Du ML, Guo BC, Liu MX, et al. Preparation and Characterization of polypropylene grafted halloysite and their compatibility effect to polypropylene/halloysite composite. *Polym J* 2006; 38: 1198–1204.
20. Baltazar-y-Jimenez A, Seviaryna I, Sain M, et al. Acoustic, tomographic, and morphological properties of bismaleimide-modified PLA green composites. *J Reinf Plast Comp* 2011; 30: 1329–1340.
21. Kucharczyk P, Sedlarik V, Miskolczi N, et al. Properties enhancement of partially biodegradable polyamide/poly-lactide blends through compatibilization with novel poly-alkenyl-poly-maleic-anhydride-amide/imide-based additives. *J Reinf Plast Comp* 2012; 31: 189–202.
22. Jiang AJ, Xi JL and Wu HW. Effect of surface treatment on the morphology of sisal fibers in sisal/poly(lactic acid) composites. *J Reinf Plast Comp* 2012; 31: 621–630.
23. Li L, Chan CM and Weng LT. The effects of specific interactions on the surface structure and composition of miscible blends of poly(vinyl alcohol) and poly(N-vinyl-2-pyrrolidone). *Polymer* 1998; 39: 2355–2360.
24. Zhu H, Du ML, Zou ML, et al. Facile and green synthesis of well-dispersed Au nanoparticles in PAN nanofibers by tea polyphenols. *J Mater Chem* 2012; 22: 9301–9307.
25. Liu SY, Chan CM, Weng LT, et al. Surface segregation in polymer blends and interpolymer complexes with increasing hydrogen bonding interactions. *Polym Sci B* 2005; 43: 1924–1930.
26. Kharchenko SB, Douglas JF, Obrzut J, et al. Flow-induced properties of nanotube-filled polymer materials. *Nat Mater* 2004; 3: 564–568.
27. Kashiwagi T, Du FM, Douglas JF, et al. Nanoparticle networks reduce the flammability of polymer nanocomposites. *Nat Mater* 2005; 4: 928–933.
28. Payne AR and Whittaker RE. Low strain dynamic properties of filled rubbers. *Rubber Chem Technol* 1971; 44: 440–478.